AEM
Journals.ASM.org

Kinetics of Ozone Inactivation of Infectious Prion Protein

Ning Ding,[a] Norman F. Neumann,[b,c] Luke M. Price,[b] Shannon L. Braithwaite,[b] Aru Balachandran,[d] Gordon Mitchell,[d] Miodrag Belosevic,[b,e] Mohamed Gamal El-Din[a]

Department of Civil and Environmental Engineering, University of Alberta, Edmonton, Alberta, Canada[a]; Department of Public Health Sciences, University of Alberta, Edmonton, Alberta, Canada[b]; Provincial Laboratory for Public Health, Edmonton, Alberta, Canada[c]; Canadian Food Inspection Agency, Ottawa, Ontario, Canada[d]; Department of Biological Sciences, University of Alberta, Edmonton, Alberta, Canada[e]

The kinetics of ozone inactivation of infectious prion protein (PrP^{Sc}, scrapie 263K) was investigated in ozone-demand-free phosphate-buffered saline (PBS). Diluted infectious brain homogenates (IBH) (0.01%) were exposed to a predetermined ozone dose (10.8 ± 2.0 mg/liter) at three pHs (pH 4.4, 6.0, and 8.0) and two temperatures (4°C and 20°C). The inactivation of PrP^{Sc} was quantified by determining the *in vitro* destruction of PrP^{Sc} templating properties using the protein misfolding cyclic amplification (PMCA) assay and bioassay, which were shown to correlate well. The inactivation kinetics were characterized by both Chick-Watson (CW) and efficiency factor Hom (EFH) models. It was found that the EFH model fit the experimental data more appropriately. The efficacy of ozone inactivation of PrP^{Sc} was both pH and temperature dependent. Based on the EFH model, *CT* (disinfectant concentration multiplied by contact time) values were determined for 2-$\log_{10}$, 3-$\log_{10}$, and 4-$\log_{10}$ inactivation at the conditions under which they were achieved. Our results indicated that ozone is effective for prion inactivation in ozone-demand-free water and may be applied for the inactivation of infectious prion in prion-contaminated water and wastewater.

Transmissible spongiform encephalopathies (TSEs) are fatal neurodegenerative diseases that are often associated with the presence of a misfolded form (PrP^{Sc}) of normal prion protein (PrP^{C}). TSEs include scrapie of sheep and goats, chronic wasting diseases (CWD) of deer and moose, bovine spongiform encephalopathy (BSE) of cows, and Creutzfeldt-Jakob disease (CJD) of human (1). Scrapie and CWD are horizontally contagious among susceptible hosts (2), whereas BSE is not contagious in cattle but transmitted through ingestion of infected bovine tissues (3). Sporadic CJD is the most common form of CJD in humans, followed by familial CJD and iatrogenic CJD in rare cases (1). The identification of a new variant CJD (vCJD), due to consumption of BSE-contaminated meat, has raised great public concerns (4). Since then, bovine tissues potentially containing high levels of PrP^{Sc} (including skull, brain, trigeminal ganglia, eyes, tonsils, spinal cord, and dorsal root ganglia of cattle aged 30 months or older, and the distal ileum of cattle of all ages) have been designated specified risk materials (SRM) and cannot be used for animal feed, pet food, or fertilizer by the industry (5). Effective inactivation and disposal of SRM is important for limiting risks posed to public health through contamination of the environment, as PrP^{Sc} is notable for its persistence in the environment (6).

Water and wastewater may act as transporting agents of infectious prions. It has been reported that PrP^{Sc} was detected in surface water samples from an area where CWD is endemic (7). Because of the possibility that SRM liquid waste may be released into the environment, there is also a possibility that infectious prions may enter wastewater treatment systems. In the case of PrP^{Sc} present in wastewater, BSE infectivity has been demonstrated to persist in raw sewage for longer than 150 days (8), and anaerobic digestion had a very limited impact on prion degradation (9), which indicates that infectious prions would survive conventional wastewater treatment.

Ozone has the highest oxidation potential among most chemical disinfectants used in water treatment (10) and has been widely used for inactivation of bacteria, viruses, and protozoa (11–14). We recently examined the effectiveness of PrP^{Sc} inactivation by ozone (15). PrP^{Sc} (scrapie 263K) was inactivated by ozone under a variety of conditions, with inactivation levels being dependent upon the applied ozone dose (7.6 to 25.7 mg/liter), contact time (5 s and 5 min), pH (pH 4.4, 6.0, and 8.0), and temperature (4 and 20°C). We reported that higher ozone doses, greater contact time (5 min), low pH (4.4), and elevated temperature (20°C) resulted in the highest level of PrP^{Sc} inactivation, as evaluated by protein misfolding cyclic amplification (PMCA). With the demonstration of the effectiveness of ozone for inactivation of PrP^{Sc} and the foundation of preliminary derivation of *CT* (disinfectant concentration multiplied by contact time) under various conditions in our previous study (15), an understanding of the kinetics of ozone inactivation of PrP^{Sc} is required for the design of competent water treatment technologies capable of inactivating infectious prions.

In this study, ozone inactivation experiments were performed with variable pHs and temperatures. Most natural waters and municipal wastewater have a pH range of 6 to 8 (16), and the pH of wastewater from slaughterhouses can be as low as 3 due to pH adjustment for blood removal (17). Therefore, we selected three pHs (4.4, 6.0, and 8.0) within this range for evaluation. Two temperatures, 4 and 20°C, were chosen to represent ambient and cold water temperatures. The applied ozone doses were regulated to be close to 10 mg/liter, allowing residual ozone to persist for 5 min under all testing conditions. These applied ozone doses were within the range for ozone disinfection of secondary municipal wastewater effluents (18). The objectives of this study were to (i) compare the fit of previously described water disinfection models for ozone inactivation of PrP^{Sc}, (ii) document the ozone inactiva-

Received 29 November 2012 Accepted 6 February 2013
Published ahead of print 15 February 2013
Address correspondence to Mohamed Gamal El-Din, mgamalel-din@ualberta.ca, or Norman F. Neumann, Norman.Neumann@albertahealthservices.ca.

doi:10.1128/AEM.03698-12

tion of PrP^{Sc} at various pHs and temperatures based on the models with the best fit, and (iii) compare the PMCA assay and animal bioassay on determination of prion inactivation by ozone.

MATERIALS AND METHODS

Ethics statement. All animal work procedures were performed under strict accordance with Canadian Council on Animal Care guidelines in such a manner as to minimize suffering. Protocols were approved and monitored by the Animal Care Committee at the Canadian Food Inspection Agency, Ottawa Laboratory—Fallowfield. Three- to six-week-old female Syrian golden hamsters (Charles River Laboratories International, Inc., Wilmington, MA) were used to prepare infectious brain homogenates (IBH) and normal brain homogenates (NBH). The detailed procedure for preparation of homogenates was described previously by Ding et al. (15).

Ozone inactivation of PrP^{Sc}. The procedures for preparation of ozone demand-free (ODF) 1× phosphate-buffered saline (PBS) (pH 4.4, pH 6.0, and pH 8.0), reaction vials, pipette tips, and magnetic bars were described previously by Ding et al. (15). Ozone stock solutions (in 1× PBS at pH 4.4, 6.0, and 8.0) were generated using ultrapure oxygen and an ozone generator (G30; PCI Wedeco). An ozone stock solution was prepared by bubbling ozone gas into 1 liter of 1× PBS for 30 min at 4°C. The ozone inactivation experiments were done by stabilizing 1.5-ml glass shell vials (Fisher Scientific, Canada) using a plastic grid box, which was submerged in ice water (4 ± 1°C) and/or directly mounted on top of a magnetic stirrer at room temperature (controlled at 20 ± 1°C). Magnets were put into each reaction vial to ensure even mixing during the reaction. Separate reaction vials were set up to withdraw samples at predetermined reaction times (3 s, 15 s, 2 min, 3 min, and 5 min). The ozone concentration in the stock solution was determined prior to the ozone inactivation experiment using a UV-visible spectrophotometer (Biospec Mini 1240; Shimadzu, Japan) at 260 nm, a molar absorption coefficient of 3,300 M^{-1} cm^{-1}, and a path length of 1 cm (19). A portion of concentrated ozone stock solution was also collected for ozone concentration determination by the indigo method at the end of the experiment (20).

The contents of reaction vessels were assembled as follows. A 10% IBH stock was diluted with 1× ODF PBS (same pH as ozone stock solution) to create a 0.1% working stock. One hundred microliters of the 0.1% IBH working stock was added to each reaction vial. Based on the known concentration of the ozone stock solution, a calculated volume of 1× ODF PBS (same pH as the ozone stock solution) was added to each reaction tube, the volume of which was intended to yield a final ozone concentration of 10.8 ± 2.0 mg/liter. The final assembled reaction in each vessel contained 0.01% IBH and ~10 mg/liter of ozone in a final volume of 1 ml. During the ozonation phase, reaction vials were covered with plastic lids. Samples from each of the vessels were withdrawn at predetermined times and assayed for residual ozone concentration by the indigo method, as described by Ding et al. (15). For the volume remaining in each of the reaction vessels, ozone activity was immediately neutralized by the addition of 20 μl of 1 M sodium thiosulfate. For positive-control samples, 20 μl of 1 M sodium thiosulfate was added to the IBH sample prior to the addition of ozone.

After ozone treatment was completed, control and ozonated samples were frozen at −80°C until PMCA was performed. The ozone inactivation experiments were performed in triplicate for each condition. All calculations of residual ozone concentrations for the ozone decomposition rate constant (k') were carried out using the readings from the indigo method only.

Quantitative analysis of inactivation. Protein misfolding cyclic amplification (PMCA), proteinase K (PK) digestion, SDS-PAGE, and Western blot analysis were conducted using procedures described by Ding et al. (15). In order to quantify the amount of PrP^{Sc} detected by Western blotting, the blots were analyzed using ImageQuant TL software (GE Healthcare). The net intensity volume of each active band was normalized by subtracting the intensity of background. Assuming that the normalized intensity volume follows an exponential relationship with dilution before reaching saturation (21), the intensity volume of all dilutions of ozonated samples and lower dilutions (−2 to −6 $\log_{10}$) of the positive-control samples were standardized against the intensity volume (saturated) of a −1-$\log_{10}$ dilution of the positive-control samples, present in the same blot image. The inactivation of PrP^{Sc} by ozonation was calculated according to equation 1:

$$\log_{10} N/N_0 = \log_{10}(\{[\log_{10}(\text{intensity of highest dilution of ozonated sample 1})/\log_{10}(\text{intensity of } -1\ \log_{10}\text{ of control})]/(\text{highest dilution of ozonated sample 1})\}/\{[\log_{10}(\text{intensity of highest dilution of control})/\log_{10}(\text{intensity of } -1\ \log_{10}\text{ of control})]/(\text{highest dilution of control})\}) \quad (1)$$

where $\log_{10}(N/N_0)$ is the $\log_{10}$ of survival of PrP^{Sc} after ozone treatment. "Intensity of highest dilution of ozonated sample 1" represents the normalized intensity volume of the signal immediately above 0 of one ozonated sample (i.e., −2-$\log_{10}$ dilution of 3-s-ozonated sample in Fig. 1). "Highest dilution of ozonated sample 1" represents the dilution with a signal immediately above 0 (in the form 10^{-n}, where n is an integer) of ozonated sample 1 (i.e., 10^{-2}). "Intensity of −1-$\log_{10}$ dilution of control" represents the normalized intensity volume of the signal of a −1 $\log_{10}$ dilution of the positive-control sample (i.e., −1-$\log_{10}$ dilution of the control in Fig. 1). "Intensity of highest dilution of control" represents the normalized intensity volume of the signal immediately above 0 of the positive-control sample (i.e., −4-$\log_{10}$ dilution of the control in Fig. 1). "Highest dilution of control" represents the dilution whose signal is immediately above 0 (in the form of 10^{-n}, where n is an integer) of the positive-control sample (i.e., 10^{-4}).

Kinetic modeling and estimation of *CT* values. The ozone decomposition rate constants, k' for each condition, were calculated using the Solver function in Microsoft Excel 2007 to regress the first-order kinetic equation

$$C = C_0 \exp(-k't) \quad (2)$$

where C and C_0 are residual ozone concentration (mg/liter) at contact time t (min) and 3 s (closest to 0 s), respectively; k' is the first-order ozone decomposition rate constant (min^{-1}). The inactivation of PrP^{Sc} under each condition grouped by pH and temperature was fit into both the Chick-Watson (CW) model and the efficiency factor Hom (EFH) model, as shown in equations 3 and 4, respectively.

$$\log_{10}\frac{N}{N_0} = -\frac{k}{k'n}C_0^n[1-\exp(-nk't)] \quad (3)$$

$$\log_{10}\frac{N}{N_0} = -kC_0^n t^m\left[\frac{1-\exp\left(-\frac{nk't}{m}\right)}{\left(\frac{nk't}{m}\right)}\right]^m \quad (4)$$

where k is the inactivation rate constant, n is the constant referred to as the coefficient of dilution, and m is the constant for the inactivation rate law which describes the deviation from the ideal Chick-Watson law. The value $\log_{10}(N/N_0)$ is as presented in equation 1, C_0, t, and k' are as presented in equation 2. To determine the unknown parameters in equations 3 and 4, the Solver function in Microsoft Excel 2007 was used to minimize the sum of squares of the differences (error sum of squares [ESS]) between observed (equation 1) and predicted (equation 3 and 4) survival under each condition.

The *CT* values were estimated for the purpose of assessing the ozone inactivation of PrP^{Sc}. Assuming that ozone decomposition follows pseudo-first-order kinetics after initial ozone demand, the *CT* values (mg · $liter^{-1}$ min) were estimated by the area under the ozone decay curve at the specific time, using equation 5.

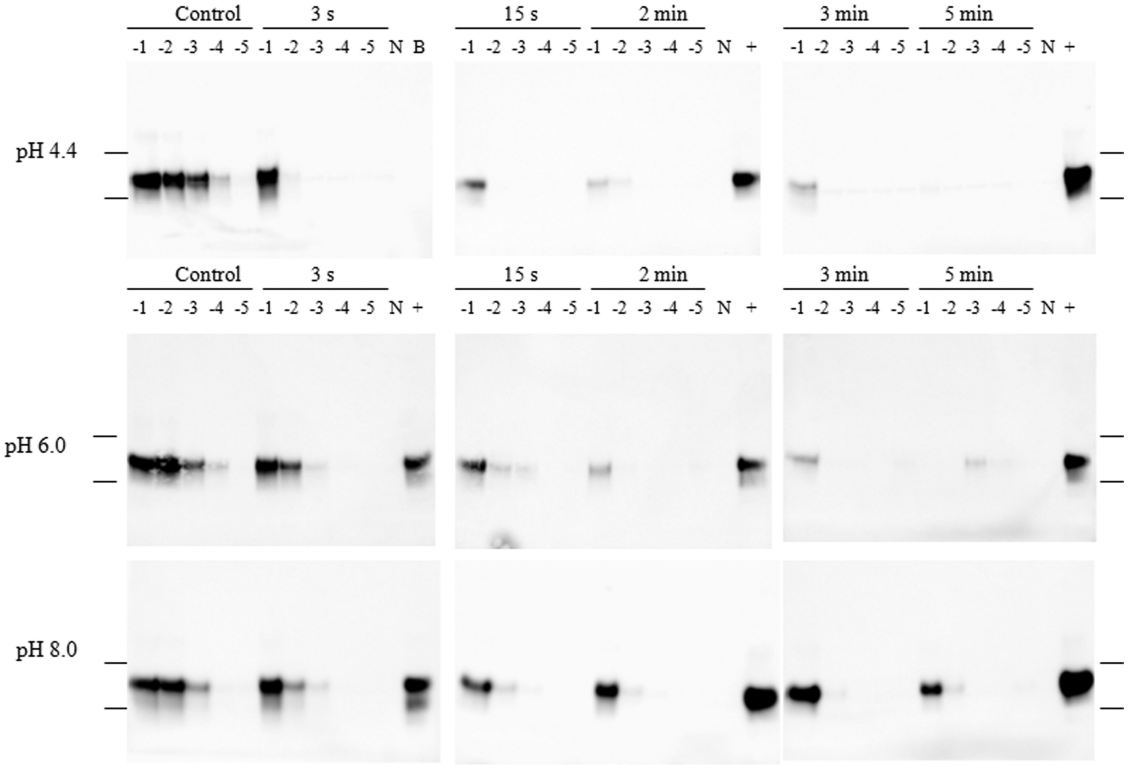

FIG 1 Western blot images of 0.01% IBH samples ozonated at 4°C and amplified by PMCA. The images in each row, from left to right, represent positive-control samples and samples treated with ozone for 3 s, 15 s, 2 min, 3 min, and 5 min. The numbers above the blots (−1 to −5) represent $\log_{10}$ dilutions of samples. N, 10% NBH treated with PK; B, blank. Lanes labeled with a plus sign contain a −1-$\log_{10}$ dilution of positive-control samples (same samples as the −1 $\log_{10}$ control in the first lane in the left column). Molecular weights of 37,000 and 25,000 are indicated on the far left and right.

$$CT = \int C(t)dt = \frac{C_o}{k'}\left[1 - \exp(-k't)\right] \quad (5)$$

where C_o, k', and t are as presented in equation 2.

Animal bioassay. Animal infectivity was used to validate PMCA results obtained from ozonation experiments. Three- to six-week-old female Syrian golden hamsters (Charles River Laboratories International Inc., Washington, MA) were used in this study. To determine infectious titers by endpoint titration, hamsters were intracranially inoculated with 50 μl of serially diluted infectious 263K brain homogenate in PBS over a range of 10^{-1} to 10^{-9}, with eight to 10 hamsters per group. Hamsters were monitored for clinical evidence of neurological disease and were euthanized when terminally affected or after >300 asymptomatic days postinoculation. Disease transmission was confirmed by immunohistochemical staining of brain sections using an automated immunostainer (Ventana Medical Systems, Tucson, AZ) and the monoclonal antibody SAF84 (Cayman Chemical, Ann Arbor, MI). The infectious titer was determined to be $10^{9.94}$ 50% infectious doses (ID_{50}) per gram of infectious brain tissue using the method of Reed and Muench (22). Infectious titers of test samples were calculated from incubation times based on standard curves generated using linear regression and four-parameter logistic regression by Sigma Plot 12 (23).

Due to the length of time required to complete the bioassay (>300 days), ozone-treated samples processed previously by Ding et al. (15) were used for validation of the PMCA assay. Groups of four to six hamsters were intracranially inoculated with control and ozone-treated samples (50 μl each), as follows: 10% NBH (bioassay-negative control), 10% IBH (bioassay-positive control), positive-control samples (0.01% IBH with quenched ozone), samples ozonated with dose of 13.7 mg/liter at 4°C and pH 4.4, samples ozonated with 13.7 mg/liter for 5 min at pH 4.4 and 4°C, samples ozonated with 12.5 mg/liter for 5 s at pH 6.0 and 4°C, samples ozonated with 12.5 mg/liter for 5 min at pH 6.0 and 4°C, samples ozonated with 14.1 mg/liter for 5 s at pH 8.0 and 4°C, and samples ozonated with 14.1 mg/liter for 5 min at pH 8.0 and 4°C. As described above, animals were euthanized and tested by immunohistochemistry if they displayed terminal disease or were asymptomatic >300 days postinoculation.

Statistical analysis. The correlation coefficient (R^2) for each kinetic model was calculated by regression (Microsoft Excel 2007) to determine the fit of the predicted CW or EFH model-of-inactivation curve to the observed inactivation data. The differences in inactivation under various conditions were analyzed by a *t* test with a 95% confidence level using GraphPad Prism 4.

RESULTS

Ozone inactivation experiments were conducted under various conditions, including different pHs (4.4, 6.0, and 8.0) and temperatures (4 and 20°C). With exposure to ozone, PrP^{Sc} templating properties were gradually inactivated over the course of 5 min of exposure (Fig. 1 and Fig. 2). At 4°C, a loss of 2 to 3 $\log_{10}$ in PrP^{Sc} signal intensity was observed after 3 s at pH 4.4, and no signal was detected after a contact time of 5 min (Fig. 1). The loss of ability of PrP^{Sc} as a seeding template for misfolding of PrP^{C} by PMCA was also observed at other pHs (pH 6.0 and 8.0) after ozone treatment; however, at pH 6.0 and 8.0, the complete loss of the seeding effect was not achieved after 5 min (Fig. 1). This is in accordance with the findings in our previous study (15). PMCA Western blot images of samples treated at 20°C are shown in Fig. 2. To generate a quantitative estimate of ozone inactivation, triplicate Western blot images were analyzed by densitometric analysis, and the val-

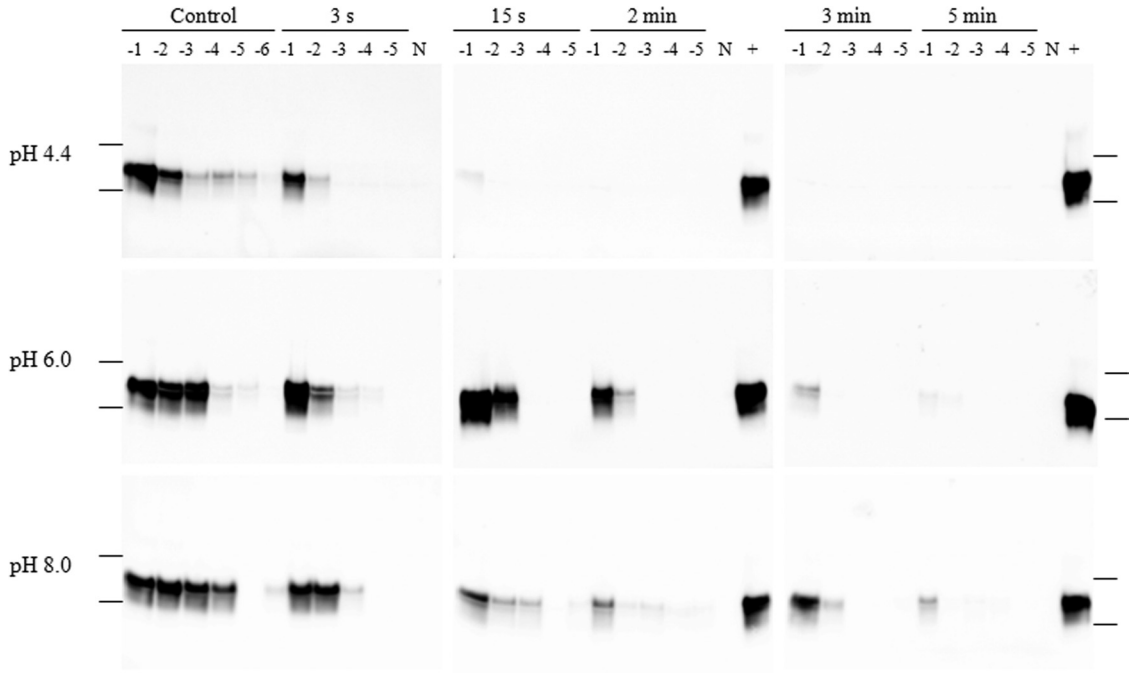

FIG 2 Western blot images of 0.01% IBH samples ozonated at 20°C and amplified by PMCA. The images in each row, from left to right, represent positive-control samples and samples treated with ozone for 3 s, 15 s, 2 min, 3 min, and 5 min. The numbers above the blots (−1 to −6) represent $\log_{10}$ dilutions of samples. N, 10% NBH treated with PK. Lanes labeled with a plus sign contain a -1-$\log_{10}$ dilution of positive-control samples (same samples as the -1 $\log_{10}$ control in the left column). Molecular weights of 37,000 and 25,000 are indicated on the far left and right.

ues for $\log_{10}(N/N_0)$ were estimated as described in Materials and Methods. Observed survival of PrP^{Sc} exposures to ozone for each testing condition is illustrated in Fig. 3.

As shown in Fig. 3, the observed survival data were characterized by an apparent rapid inactivation, followed by a tailing effect. This nonlinear appearance of survival suggested that a nonlinear model was essential for adequate description of ozone inactivation kinetics of PrP^{Sc}. Both of Chick-Watson (CW) and efficiency factor Hom (EFH) models were used to predict the inactivation kinetics. The applied ozone doses, ozone concentration (C_0; $t = 3$ s), and parameters for CW and EFH models of inactivation at each condition are provided in Table 1. The initial demand of ozone at pH 8.0 was much higher than that at other pHs, as C_0 decreased from 10.49 to 7.58 mg/liter at 4°C and from 12.54 to 7.14 mg/liter at 20°C (Table 1). It was also observed that ozone decay was fastest at pH 8.0 and 20°C ($k' = 0.36\ \text{min}^{-1}$), followed by pH 8.0 and 4°C, pH 6.0 and 20°C, and pH 4.4 and 20°C. Minimum ozone decay was observed at pH 4.4 ($k' = 0.05\ \text{min}^{-1}$) and pH 6.0 ($k' = 0.07\ \text{min}^{-1}$) at 4°C (Table 1). Compared with the CW model, the EFH model was a better fit for the observed values. For the prediction of the inactivation kinetics for all testing conditions, the ESS values of the EFH model were more than 20 times smaller than ESS values of the CW model, and the correlation coefficients (R^2) of EFH-predicted values were closer to 1 than those of the CW-predicted values (Table 1), indicating that the EFH model was more appropriate for the prediction of the inactivation of PrP^{Sc} by ozone.

Under all testing conditions in our study, the inactivation curve predicted by the EFH model steeply declined (in the first 15 s), followed by a slower tailing effect. As observed in our previous study (15), ozone inactivation of PrP^{Sc} was pH and temperature dependent. As shown in Fig. 3, the inactivation was higher at lower pH. At 4°C, the inactivation reached 2.6 $\log_{10}$ in 3 s at pH 4.4, followed by a gradual increase to >4 $\log_{10}$ in 5 min (Fig. 3A). In contrast, at pH 6.0, the inactivation was 2.0 $\log_{10}$ at 3 s and gradually increased to 3.4 $\log_{10}$ at 5 min (Fig. 3B). The inactivation at pH 8.0 was even lower, with a 0.8-$\log_{10}$ inactivation at 3 s and a 2.5-$\log_{10}$ inactivation at 5 min (Fig. 3C). Similarly, the inactivation of PrP^{Sc} was the highest at pH 4.4, followed by pH 6.0 and pH 8.0, at 20°C. The inactivation of infectious prions at various pHs was significantly different ($P < 0.05$). The ozone inactivation of PrP^{Sc} was also found to be more efficient at a high temperature (20°C) than at a low temperature (4°C). At pH 4.4, the inactivation was raised from 3.0 to 4.0 $\log_{10}$ at 15 s and from 3.5 to >5 $\log_{10}$ at 2 min, as temperature was increased from 4 to 20°C (Fig. 3A). Greater inactivation at higher temperatures was also observed at pH 6.0 and 8.0. The effect of temperature was also found to be significant for all pHs tested ($P < 0.05$) (Fig. 3B and C).

The estimated *CT* values from EFH models for ozone inactivation of PrP^{Sc} under various treatment conditions are presented in Table 2. In general, the required *CT* values were lower for higher temperatures and lower pHs. For example, to achieve a 4-$\log_{10}$ inactivation at pH 4.4, the required *CT* value for 20°C was much lower than that for 4°C. As modeled by EFH, the *CT* value was as low as 2.62 mg liter^{-1} min at pH 4.4 and 20°C, for a 4-$\log_{10}$ PrP^{Sc} inactivation. A ≥3-$\log_{10}$ inactivation could not be achieved in 5 min at pH 8.0 and 4°C, and a ≥4-$\log_{10}$ inactivation was not obtained in 5 min at pH 6.0 and 4°C or at pH 8.0 and 20°C. Overall, ozone inactivation of PrP^{Sc} was most effective at pH 4.4 and 20°C and least effective at pH 8.0 and 4°C.

To investigate whether PMCA results were associated with infectivity, ozone-treated samples were also analyzed by animal bio-

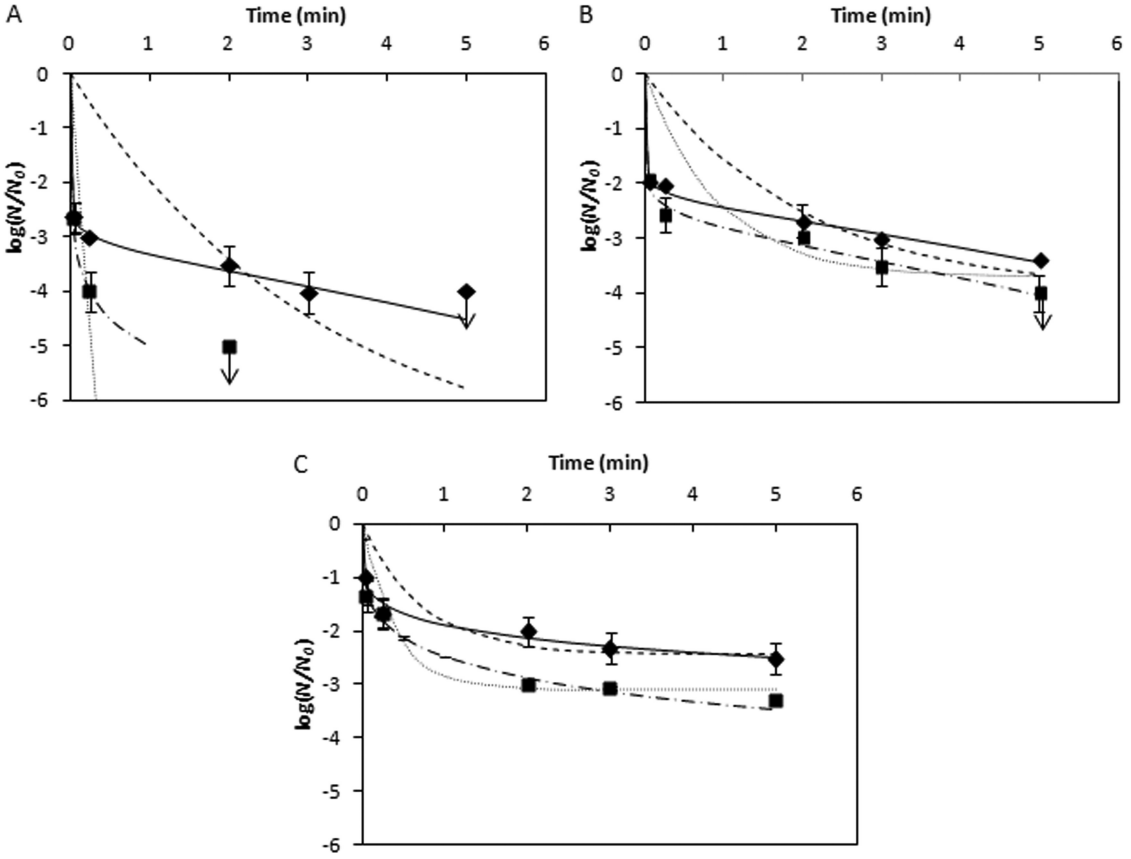

FIG 3 Inactivation of PrP^{Sc} by ozone at 4 and 20°C at pH 4.4 (A), pH 6.0 (B), and pH 8.0 (C). ◆, observed data at 4°C; ■, observed data at 20°C; —, EFH-predicted model at 4°C; –·–, EFH-predicted model at 20°C; - - -, CW-predicted model at 4°C; ···, CW-predicted model at 20°C. The arrow indicates that the values were smaller than shown.

assay. Samples that had been treated with ozone at 4°C and at three pHs (4.4, 6.0, and 8.0) and processed in our previous study (15) were examined. A linear standard curve of IBH dilution up to 0.00001% (2.94 ID_{50}/g brain; incubation time = 118 days) was generated to determine the ID_{50} of ozone-treated samples with incubation times of less than 118 days (data not shown). A four-parameter standard curve of IBH dilution up to 0.0000001% (0.94 ID_{50}/g brain; incubation time >300 days) was also plotted to determine the ID_{50} of ozone-treated samples with a latent period more than 118 days in bioassay (data not shown). By using the four-parameter standard curve, both the delay in incubation and the variation in the percentage of animals showing symptoms of illness were considered (23). The $\log_{10}$ inactivation for each treatment condition was calculated by taking the difference from read-

TABLE 1 Summary of estimated parameters for the fitted CW and EFH models

Condition	Applied ozone dose (mg/liter)	C_0 (at 3 s) (mg/liter)	k' (min^{-1})[a]	Model	k	n	m	ESS[b]	R^{2c}
pH 4.4, 4°C	11.79	10.07	0.05	CW	5.92×10^{-7}	6.57		12.58	0.95
				EFH	97.32	−1.48	0.06	0.03	0.98
pH 4.4, 20°C	12.81	10.95	0.13	CW	1.49×10^{-5}	5.92		8.30	1.00
				EFH	0.80	0.79	0.19	0.00	1.00
pH 6.0, 4°C	8.82	7.67	0.07	CW	1.14×10^{-6}	7.06		6.11	0.97
				EFH	22.88	−1.12	0.07	0.02	0.98
pH 6.0, 20°C	12.19	10.66	0.17	CW	1.14×10^{-6}	6.37		6.09	0.84
				EFH	8.11	−0.46	0.09	0.07	0.97
pH 8.0, 4°C	10.49	7.58	0.20	CW	3.42×10^{-6}	6.81		1.71	0.88
				EFH	1.86	0.01	0.17	0.07	0.95
pH 8.0, 20°C	12.54	7.14	0.36	CW	6.79×10^{-6}	7.11		1.01	0.95
				EFH	2.27	0.05	0.23	0.05	0.98

[a] Average pseudo-first-order ozone decomposition rate constant of three replicates.
[b] Error sum of squares.
[c] Correlation coefficient between predicted and observed values.

TABLE 2 Predicted *CT* values of PrP^{Sc} inactivation by ozone

Condition	Estimated *CT* (mg liter^{-1} min) at inactivation level[a]		
	2 $\log_{10}$ (99%)	3 $\log_{10}$ (99.9%)	4 $\log_{10}$ (99.99%)
pH 4.4, 4°C	0.01	3.02	30.68
pH 4.4, 20°C	0.06	0.55	2.62
pH 6.0, 4°C	0.73	22.69	NA
pH 6.0, 20°C	0.41	14.31	35.16
pH 8.0, 4°C	9.07	NA	NA
pH 8.0, 20°C	2.59	11.68	NA

[a] NA, not available under current conditions.

ings of the ID_{50} of positive-control and ozone-treated samples from the standard curve. As shown in Table 3, the reduction of infectivity of ozone-treated samples for both 5 s and 5 min at pH 4.4 and 4°C was >4.1 $\log_{10}$. The reductions of ozone-treated samples for 5 s and 5 min at pH 6.0 and 4°C were 3.1 $\log_{10}$ and 3.5 $\log_{10}$, respectively. The reductions of ozone-treated samples for both 5 s and 5 min at pH 8.0 and 4°C were 1.0 $\log_{10}$ and 3.1 $\log_{10}$, respectively. The PMCA assay data correlated with the bioassay findings to a large extent, most notably in reflecting the trends of inactivation as functions of reaction time and pHs (Table 3).

DISCUSSION

As reported in our previous study, the PMCA assay has a dynamic range of sensitivity of detection for 263K scrapie of 7 to 8 $\log_{10}$ after one round of amplification (19 h) (15), making it an amenable assay for determining inactivation kinetics of chemical disinfectants on prions. In this study, we found that the infectivity reduction evaluated by bioassay was similar to or about 1 $\log_{10}$ higher than that of PMCA assay, which corresponds with the results of another study, which also demonstrated consistency within 1 $\log_{10}$ between the two assays (24). It was recently reported that the PMCA assay may be 10^1 to 10^3 times more sensitive than the bioassay, depending on the strain of PrP^{Sc} (25, 26); however, the authors emphasized that the applicability of PMCA as a quantitative assay lies in its advantages in quantification of low-titer PrP^{Sc} and significant reduction of time and labor and more ethical animal usage (25). Furthermore, the correlation between the prion seeding activity (i.e., PMCA) and prion infectivity (i.e., animal bioassay) based on inactivation parameters such as pH, reaction time, and ozone dose, as demonstrated in our study, provides further support for the use of the PMCA assay as an effective approach for generation of prion inactivation kinetics. In this respect, modeling kinetics based on the PMCA assay appear to be valid but may conservatively underestimate the reduction of infectivity. For water and wastewater treatment engineering principles, conservative approaches or estimation is usually applied in order to ensure an extra measure of safety, especially in situations where real conditions are difficult or impossible to monitor or simulate (14). The models reported in our study best represent these situations.

To our knowledge, this is the first study describing the kinetics

TABLE 3 Comparison of infectivity reduction evaluated by bioassay and PMCA assay

Sample	Attack rate (%) (no. of clinical animals/no. animals infected)	Incubation time (days) (SD)	Infectivity reduction ($\log_{10}$)	
			Bioassay	PMCA (11)
Scrapie 263K IBH, dilution				
10^{-1}	100 (8/8)	63 (4)		
10^{-2}	100 (9/9)	77 (6)		
10^{-3}	100 (10/10)	85 (6)		
10^{-4}	100 (10/10)	86 (5)		
10^{-5}	100 (10/10)	96 (2)		
10^{-6}	100 (10/10)	103 (2)		
10^{-7}	100 (9/9)	118 (11)		
10^{-8}	22 (2/9)	219 (243, 194[a])		
10^{-9}	0 (0/10)	>300		
Bioassay negative control (10% NBH)	0/2[b]	>300		
Bioassay positive control (10% IBH)	5/5	68 (0)		
Positive control 0.01% IBH (ozone quenched with sodium thiosulfate)	6/6	89 (4)		
Ozone (13.7 mg/liter) treated for 5 s at pH 4.4 and 4°C	0/4[b]	>300	>4.1	2.8
Ozone (13.7 mg/liter) treated for 5 min at pH 4.4 and 4°C	0/2[b]	>300	>4.1	>4
Ozone (12.5 mg/liter) treated for 5 s at pH 6.0 and 4°C	5/5	124 (30)	3.1	1.9
Ozone (12.5 mg/liter) treated for 5 min at pH 6.0 and 4°C	5/6	145 (24)	3.5	3.6
Ozone (14.1 mg/liter) treated for 5 s at pH 8.0 and 4°C	6/6	97 (4)	1.0	1.1
Ozone (14.1 mg/liter) treated for 5 min at pH 8.0 and 4°C	6/6	123 (5)	3.1	2.9

[a] Incubation times for two animals.

[b] Groups each contained animals that were euthanized prior to 300 days (range, 202 to 238 days) due to illness unrelated to scrapie or that tested negative for scrapie and were not included in the calculations. The remaining hamsters had no indication of scrapie at >300 days and were PrP^{Sc} negative, as verified by immunohistochemistry after euthanasia.

of ozone inactivation of infectious prion protein. We applied the CW and EFH models, which are typically used in water disinfection under disinfectant demand conditions. Compared to the CW model, the EFH model more accurately described the initial steep inactivation curve and the tailing-off behavior for PrP^{Sc}. It has been reported that the CW model adequately describes chlorine-induced inactivation but not ozone-induced inactivation of microbes (27, 28). The Hom model accounts for the deviation from the CW model in practice (29). In the presence of obvious ozone decay during reactions, the modified Hom models (i.e., EFH) provided the best fit for viral, protozoan, and bacterial inactivation by ozone in water (30–32). The tailing effect observed in these studies was attributed to clumping of organisms, the presence of pathogen subpopulations with various degrees of resistance to the disinfectant, or distributed resistance within a single population (33, 34).

Like viruses, prions lack certain biological characteristics directly associated with self-maintenance and replication and therefore require infection of a living tissue. Prions were once considered "protein only" (1), but studies have shown that cofactors such as RNA and lipids might also be components of the infectious particles (35, 36). The conformational misfolding of PrP^{C} to PrP^{Sc} results in an increase in β-sheet content (37), which causes the protein to aggregate and makes it resistant to regular disinfectants. Ozone has been reported to target susceptible amino acids, such as cysteine, methionine, tryptophan, tyrosine, histidine, cystine, and phenylalanine, affecting the primary structure of the infectious prion protein (38). The oxidation and cleavage of selected amino acids or monomeric units can induce modifications of the primary structure or significant changes in the secondary, tertiary, and quaternary structure or hinder protein folding abilities (39).

The effect of pH on PrP^{Sc} inactivation by ozone was significant ($P < 0.05$) at both 4 and 20°C, and PrP^{Sc} was inactivated more rapidly at pH 4.4 than at pH 6.0 and 8.0. The effect of pH on ozone inactivation of microorganisms in water has been investigated for a variety of water pathogens. In some studies, the effect of pH has been reported to be insignificant for ozone inactivation of *Cryptosporidium parvum* oocysts at pH 6 to 10 (40–43) and poliovirus at pH 3 to 10 (44). However, ozone was also reported to be more effective for *Giardia muris* cysts (45) and *Bacillus subtilis* spores (46–48), with inactivation being greater at higher pH (pH 5 to 10). While our data are distinct from those of studies which demonstrated greater inactivation at higher pH (46–48), ozone inactivation of *Escherichia coli* and norovirus has also been shown to be more effective at a lower pH (32, 49). Thus, the pH effect for ozone inactivation appears to be microorganism specific and is likely to be dependent on the structural components of the microorganisms (45).

In addition to the pH specificity of ozone against various microorganisms, one of the most important factors affecting pH during ozonation is the application and interpretation of ozone doses. The variance of applied ozone doses may directly lead to the difference of inactivation (15, 45, 50). Farooq et al. reported that ozone inactivation of *Mycobacterium fortuitum* was higher at pH 5.7 than at pH 10.1 with similar applied ozone doses, while the difference was insignificant when residual ozone concentrations were maintained at similar levels (51). It was suggested that the high inactivation rate was due to the lower ozone decay rate at lower pH (52). In our study, the applied ozone doses at various pHs were at the same level, which indicated that low pH favored molecular ozone and acted as the major oxidant for PrP^{Sc} inactivation. At a pH above 4, ozone gradually decomposes into hydroxyl radicals ($^{\bullet}OH$) with the initiator of OH^{-} in a chain reaction (52), as outlined in equations 6 and 7.

$$O_3 + OH^- \rightarrow HO_2^- + O_2 \quad (6)$$

$$O_3 + HO_2^- \rightarrow {}^{\bullet}OH + O_2^{\bullet -} + O_2 \quad (7)$$

It was shown that $^{\bullet}OH$ was generated by O_3 in reaction with OH^{-} in water, and the reactions were expedited as pH increased (52). Our study indicates that $^{\bullet}OH$ formed by O_3 decomposition is less effective than molecular O_3 in inactivating PrP^{Sc}. With the demonstration that the conformational stability of infectious prion agent is not affected over a pH range of 2 to 10 (53), our data suggest that oxidation of infectious prion agents by molecular ozone is more effective than indirect oxidation associated with ozone decomposition to hydroxyl ions ($^{\bullet}OH$).

Temperature has effects on ozone solubility in water, ozone decomposition rate, and inactivation rate. Under similar conditions (i.e., water characteristics and applied ozone doses), ozone decays faster at higher temperatures (Table 1) (47). However, ozone inactivation of microorganisms in water has been reported to be even higher at higher temperatures. Ozone inactivation of *Giardia lamblia* at pH 7 (45), *Naegleria gruberi* at pH 7 (45), *Cryptosporidium* at pH 6 to 8 (41, 42), and *Bacillus subtilis* spores at pH 7 (48) was higher as temperature increased toward 25°C, which is consistent with ozone inactivation of PrP^{Sc} observed in this study.

Inactivation of prions by other oxidants has also been examined in various studies (23, 54–61). Chlorine and hydroxyl radicals are the primary oxidants in these studies. It has been reported that a 4.4-$\log_{10}$ inactivation of scrapie was obtained with a 30-min exposure to residual chlorine at 1,000 mg/liter (55), which is much higher than the concentration used in water disinfection and the concentration of ozone applied in this study. A UV-ozone treatment system, which primarily generated hydroxyl radicals as oxidants, was used to treat infectious prions (54). Although more than a 5-$\log_{10}$ inactivation was achieved, the exposure time was up to 2 weeks. Other studies also demonstrated that hydroxyl radicals inactivated infectious prions, more or less, with exposure times from 30 min to several hours (23, 56, 57, 59, 60, 62). However, none of these studies investigated the reaction kinetics. In these studies, infectious brain homogenates were mixed with oxidants at predetermined concentrations, followed by a period of incubation. The effectiveness of oxidants was assessed at the end of the reaction, with or without neutralizing the oxidants. This is a biological rationale for analyzing the effectiveness of prion inactivation, without considering consumption of oxidants as a function of time. In the present study, we measured residual ozone at each reaction time point and took ozone decomposition into account in the generation of inactivation curves, which is imperative in water disinfection engineering studies.

Due to the lack of fast and sensitive detection methods, prions had not been reported in water and wastewater until the development of PMCA. CWD has been detected at very low concentrations in the water samples from one stream and the nearby water treatment plant of an area where CWD is endemic (7). In our study, the PrP^{Sc} was spiked at a concentration that, although lower than that in some prion decontamination studies (58), was higher than what might be expected in real situations during water and

wastewater treatment. Our results indicate that ozone can be used for the inactivation of infectious prion protein in surface water or an aqueous environment with limited ozone demand and lay a foundation for understanding the inactivation of infectious prions using ozone in more complex water matrices. Rendering plants generate large volumes of wastewater that may contain infectious prion protein. While blood collection is strictly regulated to ensure no contamination with SRM (63) and all SRM are required to be destroyed (i.e., through controlled incineration) or permanently contained (i.e., landfill) (64), the disposal of the wastewater generated from the same processes that render SRM is not regulated. Ozone technology, as discussed above, may serve as a barrier for prions present in wastewater from slaughterhouses or SRM rendering facilities.

In contrast to clean water and ozone demand-free buffered systems, wastewater from rendering plants contains grease, oil, and other organics which lead to high levels of ozone demand. Discharges from rendering plants without SRM are usually pretreated with screening, gravity separation, flow equalization, chemical pretreatment, and dissolved-air flotation, followed by biological treatment (65). However, with the concern of infectious prion contamination and the additional cost of disposal of sediments and floats, the ozone treatment should be added as an additional barrier to the overall process of treating wastewater generated from SRM rendering. Due to the higher biological oxygen demand (BOD) and/or chemical oxygen demand (COD) (i.e., carbonaceous BOD between 4,000 and 10,000 mg/liter) in the rendering wastewater (65), high applied ozone doses would be needed for an appropriate level of inactivation of PrP^{Sc}, depending on the characteristics of the organics and competitive reactions in the wastewater. Ozone technology has been tested for wastewater treatment having high organic content, such as olive mill wastewater (COD $\approx$ 300,000 mg/liter) in a semibatch reactor (66). Ozone has also been applied to treat diluted landfill leachate (COD = 1,010 mg/liter; BOD = 186 mg/liter). The initial feed gas ozone concentration of 8.3 mg/liter (33.3 mg/min) resulted in effective inactivation after 2 h of contact (67). From this information it is predicted that when ozone is used for inactivation of PrP^{Sc} in rendering plant wastewater, a long reaction time will be required for effective inactivation. On an industrial scale, the rate capacity of a typical oxygen-fed ozone generator in a wastewater treatment plant is around 3,000 kg/day (68), and ozone production can be further enhanced by increasing the ozone mass transfer rate, using multijet ozone contactors in continuous flow reactors (69). Therefore, full-scale ozonation systems used for industrial wastewater treatment may hold promise for controlling prion contaminated wastewater from SRM rendering facilities.

Ozone may also be a potential treatment for sterilization of medical instruments contaminated with prions in hospitals. Transmission of CJD due to neurosurgical instruments and intracerebral electrodes contamination has been documented (70); consequently, regulatory preventative methods have been proposed, including using disposable instruments or decontamination by stringent methods (71). The decontamination methods usually involve high temperatures and/or high concentrations of sodium hydroxide or bleach, which may not be appropriate for sensitive medical instruments. Alternative methods have been proposed, including Fenton reaction (23), gaseous hydrogen peroxide (72), enzymatic treatment (73), and other organic chemical treatment (74). These methods require either long reaction times (i.e., >30 min to several hours) or pretreatment and/or sequential treatment to obtain optimum inactivation levels (i.e., >5 $\log_{10}$). Due to the ability of ozone to inactivate prions in a short time, the application of ozone to medical instruments may also be feasible with further research.

In conclusion, ozone inactivation of PrP^{Sc} (scrapie 263K) in ozone demand-free phosphate-buffered saline was more accurately modeled by the efficiency factor Hom model than the Chick-Watson model. The survival curves showed a rapid inactivation followed by a tailing effect. The effects of both pH and temperature on ozone inactivation efficacy were significant ($P < 0.05$), and ozone was found to be more effective at a low pH (4.4) and high temperature (20°C). Further studies on PrP^{Sc} inactivation in complex water matrices (SRM wastewater) and PrP^{Sc}-contaminated medical instruments are needed to test ozone application in various areas.

ACKNOWLEDGMENTS

This research was financially supported by the Alberta Prion Research Institute (APRI) and PrioNet Canada through grants provided to M.B., N.F.N., and M.G.E.-D. and through a Natural Sciences and Engineering Research Council of Canada (NSERC) Discovery Accelerator Grant to M.G.E.-D.

We are grateful to Pamela Chelme-Ayala for her critical review of the manuscript. We thank Judd Aiken, Debbie McKenzie and their group at University of Alberta for sharing their PMCA sonicators with us. We are grateful to Allen Herbst for his discussion with us. We also thank the personnel at the Center for Prion and Protein Misfolding Diseases (CPPFD) at the University of Alberta for providing us the level 2+ enhanced containment laboratory to perform the experiments. We acknowledge the exceptional support from staff in the Transmissible Spongiform Encephalopathy Unit and the Animal Care Facility at the Ottawa Laboratory Fallowfield, particularly Antanas Staskevicius and Patricia Shaffer.

REFERENCES

1. **Prusiner SB.** 1998. Prions. Proc. Natl. Acad. Sci. U. S. A. **95**:13363–13383.
2. **Smith CB, Booth CJ, Pedersen JA.** Fate of prions in soil: a review. J. Environ. Qual. **40**:449–461.
3. **Wilesmith JW, Ryan JBM, Atkinson MJ.** 1991. Bovine spongiform encephalopathy—epidemiologic studies on the origin. Vet. Rec. **128**:199–203.
4. **Will RG, Cousens SN, Farrington CP, Smith PG, Knight RSG, Ironside JW.** 1999. Deaths from variant Creutzfeldt-Jakob disease. Lancet **353**:979.
5. **Canadian Food Inspection Agency.** 2011. The Canadian Food Inspection Agency (CFIA) position on head hides (face plates) from cattle slaughtered in Canadian abattoirs. http://www.inspection.gc.ca/english/anima/disemala/bseesb/enhren/heatete.shtml.
6. **Pedersen JA, McMahon KD, Benson CH.** 2006. Prions: novel pathogens of environmental concern? J. Environ. Eng. ASCE **132**:967–969.
7. **Nichols TA, Pulford B, Wyckoff AC, Meyerett C, Michel B, Gertig K, Hoover EA, Jewell JE, Telling GC, Zabel MD.** 2009. Detection of protease-resistant cervid prion protein in water from a CWD-endemic area. Prion **3**:171–183.
8. **Maluquer de Motes C, Espinosa JC, Esteban A, Calvo M, Girones R, Torres JM.** 2012. Persistence of the bovine spongiform encephalopathy infectious agent in sewage. Environ. Res. **117**:1–7.
9. **Hinckley GT, Johnson CJ, Jacobson KH, Bartholomay C, McMahon KD, McKenzie D, Aiken JM, Pedersen JA.** 2008. Persistence of pathogenic prion protein during simulated wastewater treatment processes. Environ. Sci. Technol. **42**:5254–5259.
10. **US Environmental Protection Agency.** 1999. Alternative disinfectants and oxidants. http://www.epa.gov/ogwdw/mdbp/alternative_disinfectants_guidance.pdf.
11. **Hoff JC.** 1986. Inactivation of microbial agents by chemical disinfectants. Water Engineering Research Laboratory, US Environmental Protection Agency, Washington, DC.
12. **Thurston-Enriquez JA, Haas CN, Jacangelo J, Gerba CP.** 2005. Inacti-

vation of enteric adenovirus and feline calicivirus by ozone. Water Res. **39**:3650–3656.
13. **US Environmental Protection Agency.** 1991. Guidance manual for compliance with the filtration and disinfection requirements for public water systems using surface water sources. http://www.epa.gov/safewater/mdbp/guidsws.pdf.
14. **US Environmental Protection Agency.** 2006. National Primary Drinking Water Regulations: long term 2 enhanced surface water treatment. http://www.epa.gov/safewater/disinfection/lt2/pdfs/guide_lt2_stateimplementation.pdf.
15. **Ding N, Neumann NF, Price LM, Braithwaite SL, Balachandran A, Belosevic M, El-Din MG.** 2012. Inactivation of template-directed misfolding of infectious prion protein by ozone. Appl. Environ. Microbiol. **78**:613–620.
16. **Spellman FR.** 2009. Handbook of water and wastewater treatment plant operations, 2nd ed. CRC Press, Boca Raton, FL.
17. **Masse DI, Masse L.** 2000. Characterization of wastewater from hog slaughterhouses in Eastern Canada and evaluation of their in-plant wastewater treatment systems. Can. Agr. Eng. **42**:139–146.
18. **Paraskeva P, Graham NJD.** 2002. Ozonation of municipal wastewater effluents. Water Environ. Res. **74**:569–581.
19. **Hart EJ, Sehested K, Holcman J.** 1983. Molar absorptivities of ultraviolet and visible bands of ozone in aqueous solutions. Anal. Chem. **55**:46–49.
20. **American Public Health Association.** 2005. Standard methods for the examination of water and wastewater, 21st ed. American Public Health Association, Washington, DC.
21. **Saborio GP, Permanne B, Soto C.** 2001. Sensitive detection of pathological prion protein by cyclic amplification of protein misfolding. Nature **411**:810–813.
22. **Reed LJ, Muench H.** 1938. A simple method of estimating fifty per cent endpoints. Am. J. Hyg. **27**:493–497.
23. **Lehmann S, Pastore M, Rogez-Kreuz C, Richard M, Belondrade M, Rauwel G, Durand F, Yousfi R, Criquelion J, Clayette P, Perret-Liaudet A.** 2009. New hospital disinfection processes for both conventional and prion infectious agents compatible with thermosensitive medical equipment. J. Hosp. Infect. **72**:342–350.
24. **Pritzkow S, Wagenfuhr K, Daus ML, Boerner S, Lemmer K, Thomzig A, Mielke M, Beekes M.** 2011. Quantitative detection and biological propagation of scrapie seeding activity in vitro facilitate use of prions as model pathogens for disinfection. PLoS One **6**:e20384. doi:10.1371/journal.pone.0020384.
25. **Makarava N, Savtchenko R, Alexeeva I, Rohwer RG, Baskakov IV.** 2012. Fast and ultrasensitive method for quantitating prion infectivity titre. Nat. Commun. **3**:741.
26. **Wilham JM, Orru CD, Bessen RA, Atarashi R, Sano K, Race B, Meade-White KD, Taubner LM, Timmes A, Caughey B.** 2010. Rapid end-point quantitation of prion seeding activity with sensitivity comparable to bioassays. PLoS Pathog. **6**:e1001217. doi:10.1371/journal.ppat.1001217.
27. **Finch GR, Smith DW, Stiles ME.** 1988. Dose-response of *Escherichia coli* in ozone demand-free phospahte buffer. Water Res. **22**:1563–1570.
28. **Katzenelson E, Kletter B, Shuval HI.** 1974. Inactivation kinetics of viruses and bacteria in water by use of ozone. J. Am. Water Works Assoc. **66**:725–729.
29. **Hom LW.** 1972. Kinetics of chlorine disinfection in an ecosystem. J. Sanit. Eng. Div. ASCE **98**:183–194.
30. **Gyurek LL, Finch GR.** 1998. Modeling water treatment chemical disinfection kinetics. J. Environ. Eng. ASCE **124**:783–793.
31. **Haas CN, Kaymak B.** 2003. Effect of initial microbial density on inactivation of *Giardia muris* by ozone. Water Res. **37**:2980–2988.
32. **Lim MY, Kim JM, Lee JE, Ko G.** 2010. Characterization of ozone disinfection of murine norovirus. Appl. Environ. Microbiol. **76**:1120–1124.
33. **Cerf O.** 1977. Tailing of survival curves of bacterial spores. J. Appl. Bacteriol. **42**:1–19.
34. **Hiatt CW.** 1964. Kinetics of inactivation of viruses. Bacteriol. Rev. **28**:150–163.
35. **Piro JR, Supattapone S.** 2010. Photodegradation illuminates the role of polyanions in prion infectivity. Prion **5**:49–51.
36. **Wang F, Wang X, Yuan CG, Ma J.** 2010. Generating a prion with bacterially expressed recombinant prion protein. Science **327**:1132–1135.
37. **Pan KM, Baldwin M, Nguyen J, Gasset M, Serban A, Groth D, Mehlhorn I, Huang Z, Fletterick RJ, Cohen FE.** 1993. Conversion of alpha-helices into beta-sheets features in the formation of the scrapie prion proteins. Proc. Natl. Acad. Sci. U. S. A. **90**:10962–10966.
38. **Mudd JB, Leavitt R, Ongun A, McManus TT.** 1969. Reaction of ozone with amino acids and proteins. Atmos. Environ. **3**:669–681.
39. **Cataldo F.** 2006. Ozone degradation of biological macromolecules: proteins, hemoglobin, RNA, and DNA. Ozone Sci. Eng. **28**:317–328.
40. **Gyurek LL, Li HB, Belosevic M, Finch GR.** 1999. Ozone inactivation kinetics of *Cryptosporidium* in phosphate buffer. J. Environ. Eng. ASCE **125**:913–924.
41. **Li H, Gyurek LL, Finch GR, Smith DW, Belosevic M.** 2001. Effect of temperature on ozone inactivation of *Cryptosporidium parvum* in oxidant demand-free phosphate buffer. J. Environ. Eng. ASCE **127**:456–467.
42. **Ran ZL, Li SF, Huang JL, Yuan YX, Cui CW, Williams CD.** 2010. Inactivation of *Cryptosporidium* by ozone and cell ultrastructures. J. Environ. Sci. China **22**:1954–1959.
43. **Rennecker JL, Kim JH, Corona-Vasquez B, Marinas BJ.** 2001. Role of disinfectant concentration and pH in the inactivation kinetics of *Cryptosporidium parvum* oocysts with ozone and monochloramine. Environ. Sci. Technol. **35**:2752–2757.
44. **Katzenelson E, Koerner G, Biedermann N, Peleg M, Shuval HI.** 1979. Measurement of the inactivation kinetics of poliovirus by ozone in a fast-flow mixer. Appl. Environ. Microbiol. **37**:715–718.
45. **Wickramanayake GB, Rubin AJ, Sproul OJ.** 1984. Inactivation of *Naegleria* and *Giardia* cysts in water by ozonation. Water. Pollut. Control Fed. J. **56**:983–988.
46. **Cho M, Chung H, Yoon J.** 2003. Disinfection of water containing natural organic matter by using ozone-initiated radical reactions. Appl. Environ. Microbiol. **69**:2284–2291.
47. **Dow SM, Barbeau B, von Gunten U, Chandrakanth M, Amy G, Hernandez M.** 2006. The impact of selected water quality parameters on the inactivation of *Bacillus subtilis* spores by monochloramine and ozone. Water Res. **40**:373–382.
48. **Larson MA, Mariñas BJ.** 2003. Inactivation of *Bacillus subtilis* spores with ozone and monochloramine. Water Res. **37**:833–844.
49. **Zuma F, Lin J, Jonnalagadda SB.** 2009. Ozone-initiated disinfection kinetics of *Escherichia coli* in water. J. Environ. Sci. Health Part A **44**:48–56.
50. **Uhm H, Lee H, Seong BL.** 2009. Inactivation of H_1N_1 viruses exposed to acidic ozone water. Appl. Phys. Lett. **95**:173704.
51. **Farooq S, Chian ESK, Engelbrecht RS.** 1977. Basic concepts in disinfection with ozone. Water Poll. Control Fed. J. **49**:1818–1831.
52. **Langlais B, Reckhow DA, Brink DR.** 1991. Ozone in water treatment: application and engineering: cooperative research report. Lewis Publishers, Chelsea, MI.
53. **Mould DL, Dawson AM, Smith W.** 1965. Scrapie in mice. Stability of agent to various suspending media pH and solvent extraction. Res. Vet. Sci. **6**:151–154.
54. **Johnson C, Gilbert P, McKenzie D, Pedersen J, Aiken J.** 2009. Ultraviolet-ozone treatment reduces levels of disease-associated prion protein and prion infectivity. BMC Res. Notes **2**:121–125.
55. **Kimberlin RH, Walker CA, Millson GC, Taylor DM, Robertson PA, Tomlinson IH, Dickinson AG.** 1983. Disinfection studies with two strains of mouse-passaged scrapie agent. J. Neurol. Sci. **59**:355–369.
56. **Paspaltsis I, Berberidou C, Poulios I, Sklaviadis T.** 2009. Photocatalytic degradation of prions using the photo-Fenton reagent. J. Hosp. Infect. **71**:149–156.
57. **Paspaltsis I, Kotta K, Lagoudaki R, Grigoriadis N, Poulios I, Sklaviadis T.** 2006. Titanium dioxide photocatalytic inactivation of prions. J. Gen. Virol. **87**:3125–3130.
58. **Rutala WA, Weber DJ.** 2001. Creutzfeldt-Jakob disease: Recommendations for disinfection and sterilization. Clin. Infect. Dis. **32**:1348–1356.
59. **Solassol J, Pastore M, Crozet C, Perrier V, Lehmann S.** 2006. A novel copper-hydrogen peroxide formulation for prion decontamination. J. Infect. Dis. **194**:865–869.
60. **Suyama K, Yoshioka M, Akagawa M, Murayama Y, Horii H, Takata M, Yokoyama T, Mohri S.** 2007. Assessment of prion inactivation by Fenton reaction using protein misfolding cyclic amplification and bioassay. Biosci. Biotechnol. Biochem. **71**:2069–2071.
61. **Taylor DM, Fraser H, McConnell I, Brown DA, Brown KL, Lamza KA, Smith GRA.** 1994. Decontamination studies with the agents of bovine spongiform encephalopathy and scrapie. Arch. Virol. **139**:313–326.
62. **Solassol J, Arlotto M, Lehmann S.** 2004. Detection of prion after decontamination procedures: comparative study of standard Western blot, filter retention and scrapie-cell assay. J. Hosp. Infect. **57**:156–161.

63. **Canadian Food Inspection Agency.** 18 July 2007, posting date. The Canadian food inspection agency (CFIA) position on blood collection during slaughter. http://www.inspection.gc.ca/english/anima/disemala/bseesb/enhren/blosane.shtml.
64. **Canadian Food Inspection Agency.** 13 October 2007, posting date. Enhanced feed ban decision documents. http://www.inspection.gc.ca/english/anima/heasan/disemala/bseesb/enhren/enhrene.shtml.
65. **Sindt GL.** 2006. Environmental issues in the rendering industry, p 245–258. *In* Meeker DL (ed), Essential rendering. Kirby Lithographic Company Inc., Arlington, VA.
66. **Bettazzi E, Caretti C, Caffaz S, Azzari E, Lubello C.** 2007. Oxidative processes for olive mill wastewater treatment. Water Sci. Technol. **55**: 79–87.
67. **Zouboulis A, Samaras P, Ntampou X, Petala M.** 2007. Potential ozone applications for water/wastewater treatment. Separ. Sci. Techonol. **42**: 1433–1446.
68. **US Environmental Protection Agency.** 1999. Wastewater technology fact sheet—ozone disinfection. http://water.epa.gov/scitech/wastetech/upload/2002_06_28_mtb_ozon.pdf.
69. **Baawain MS, El-Din MG, Smith DW, Mazzei A.** 2011. Hydrodynamic characterization and mass transfer analysis of an in-line multi-jets ozone contactor. Ozone Sci. Eng. **33**:1–14.
70. **Brown P, Gibbs CJ, Rodgers-Johnson P, Asher DM, Sulima MP, Bacote A, Goldfarb LG, Gajdusek DC.** 1994. Human spongiform encephalopathy—the National Institutes of Health series of 300 cases of experimentally transmitted disease. Ann. Neurol. **35**:513–529.
71. **WHO.** 1999. Infection control guidelines for transmission spongiform encephalopathies. World Health Organization report, 23–26 March 1999. WHO/CDS/CSR/APH/2000.3. World Health Organization, Geneva, Switzerland.
72. **Fichet G, Antloga K, Comoy E, Deslys JP, McDonnell G.** 2007. Prion inactivation using a new gaseous hydrogen peroxide sterilisation process. J. Hosp. Infect. **67**:278–286.
73. **Jackson GS, McKintosh E, Flechsig E, Prodromidou K, Hirsch P, Linehan J, Brandner S, Clarke AR, Weissmann C, Collinge J.** 2005. An enzyme-detergent method for effective prion decontamination of surgical steel. J. Gen. Virol. **86**:869–878.
74. **Peretz D, Supattapone S, Giles K, Vergara J, Freyman Y, Lessard P, Safar JG, Glidden DV, McCulloch C, Nguyen HOB, Scott M, DeArmond SJ, Prusiner SB.** 2006. Inactivation of prions by acidic sodium dodecyl sulfate. J. Virol. **80**:322–331.